International Journal of GEOMATE, Jan., 2023, Vol.24, Issue 101, pp.1-11
ISSN: 2186-2982 (P), 2186-2990 (O), Japan, DOI: https://doi.org/10.21660/2023.101.3574
Geotechnique, Construction Materials and Environment

SAFETY EVALUATION OF OLD-STANDARD RIGID PVC PIPES WITH ADHESIVE JOINTS IN THE EVENT OF FAULT DISPLACEMENT

*Aiko Furukawa[1], Akira Ito[2], Kyosuke Asano[1] and Masaru Okutsu[2]

[1]Department of Urban Management, Kyoto University, Japan; [2] NTT Access Network Service Systems Laboratories, Japan

*Corresponding Author, Received: 31 Aug. 2022, Revised: 25 Nov. 2022, Accepted: 16 Dec. 2022

ABSTRACT: Many old telecommunication pipes built during the 1960s and 1970s are still in use in Japan. Past earthquake surveys have found that old-standard rigid polyvinyl chloride (PVC) pipes with adhesive joints are vulnerable to earthquakes, and it appears that such pipes were damaged by fault displacement during the 2016 Kumamoto earthquake. However, the safety of old-standard rigid PVC pipes in the event of fault displacement has not been evaluated. The present study evaluated the safety of old-standard PVC pipes in the event of fault displacement in finite element analysis. First, an analysis model of a pipe with an adhesive joint was developed in the numerical analysis of a bending test. An analysis model of the soil–pipe interaction was then developed in a numerical analysis of a soil-tank test. It was confirmed that the results of the bending test and the soil-tank test were accurately reproduced using the developed model. After confirming that the analysis results agree well with experimental results, a numerical analysis of the safety evaluation in the event of fault displacement was conducted. The results showed that when the joint center was located 300 mm from the fault plane where the maximum principal stress occurs and when the fault plane is perpendicular to the pipes, the yielding occurred with the smallest fault displacement of 55 mm for the new pipe and only 25 mm for removed pipes. The analysis showed that even a small displacement may cause serious damage to the old-standard rigid PVC pipes with an adhesive joint.

Keywords: Rigid PVC pipe with adhesive joint, Fault displacement, New pipe, Removed pipe, FEM

1. INTRODUCTION

Telecommunication systems are essential lifelines for daily life, and it is desirable to maintain their functions not only in normal times but also during and immediately after earthquakes. The total length of telecommunication pipes that accommodate telecommunication cables is more than 600,000 km in Japan, with most of the pipes being made to old standards in the 1960s and 1970s, during a period of high economic growth [1]. Pipes built after the 1980s have seismic joints; for example, a telescopic pipe joint. However, pipes built to old standards have joints that are different from those built to current standards and have poor seismic performance. Old-standard rigid polyvinyl chloride (PVC) pipes are rigidly connected to joints with adhesives, and the joints thus do not have a telescopic function. As a result, the pipes may be damaged in the event of large earthquakes, causing interference to telecommunication cables [2]. In a recent case, old-standard rigid PVC pipes were damaged near to where a fault displacement was observed during the 2016 Kumamoto earthquake [3].

Although not focusing on old-standard rigid PVC pipes, past studies have investigated the effect of fault displacement on pipes. Newmark and Hall [4] and Kennedy et al. [5] derived formulas for determining the strain acting on pipes due to fault displacement. Takada et al. [6] proposed a design method that simply estimates the maximum strain acting on pipes due to fault displacement. Miyajima et al. [7] and Takada et al. [8] investigated a rigid PVC pipe subjected to fault displacement. Additionally, Miyajima et al. [7] examined the effects of fault displacement on a rigid PVC pipe in soil-tank tests focusing on characteristics of the surface soil. Hassani and Basirat [9] performed a sensitivity analysis of polyethylene buried pipes subjected to faulting using FDM. Tsatis et al. [10] performed a parametric study of pipelines subjected to normal or reverse faulting using FEM. However, they considered a pipe without joints. Takada et al. [8] applied stepwise ground subsidence to a pipe with a seismic joint to understand the behavior of the joint and pipe. However, they studied a pipe with a telescopic pipe joint and not an adhesive joint.

When limited to rigid PVC pipes with adhesive joints, which are common for old-standard telecommunication pipes, no study has evaluated safety in the event of fault displacement.

The present study evaluated the safety of rigid

PVC pipes with an adhesive joint in the event of fault displacement in a three-dimensional finite element analysis. To develop an adequate analysis model of PVC pipes with an adhesive joint, the bending test of Okutsu et al. [11] was conducted for newly fabricated pipes and old pipes removed from the ground. The soil-tank test of Okutsu et al. [12] was conducted to develop an adequate analysis model for the soil–pipe interaction. The rationale of the modeling methods was proved by showing the agreement between the experimental and analysis results. After developing an adequate analysis model for pipes with an adhesive joint and soil–pipe interaction, the structural safety of old-standard rigid PVC pipes in the event of fault displacement was evaluated.

2. RESEARCH SIGNIFICANCE

No studies have focused on the safety of old-standard rigid PVC pipes with adhesive joints in the event of fault displacement. However, past earthquake surveys have found that such pipes were damaged by fault displacement during the 2016 Kumamoto earthquake. This study thus evaluates the safety of old-standard rigid PVC pipes in the event of fault displacement in a detailed three-dimensional finite element analysis. The significance of this study is that the safety of pipes against fault displacement is quantitatively evaluated for the first time based on a detailed model considering separation of adhesive joint and failure of PVC material.

3. DEVELOPMENT OF AN ANALYSIS MODEL OF RIGID PVC PIPES WITH AN ADHESIVE JOINT THROUGH SIMULATION OF A BENDING TEST

3.1 Overview

This section describes the development of an adequate analysis model of rigid PVC pipes with an adhesive joint. A three-dimensional finite element analysis was performed for the bending test conducted by Okutsu et al. [11], and the validity of the analysis model was verified by confirming the agreement of the experimental and analytical results.

3.2 Bending Test Conducted in the Past Study

The bending test [11] was conducted for rigid PVC pipes with an adhesive joint. Figure 1(a) is a photograph of a test specimen. The two pipes were connected by a joint. The pipes and joint were made from PVC and glued together. Figure 1(b) is a schematic of an adhesive joint with a pipe inserted on the left side, with dimensions given.

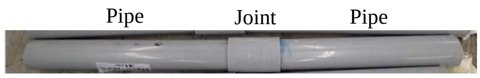

(a) Photograph of a test specimen

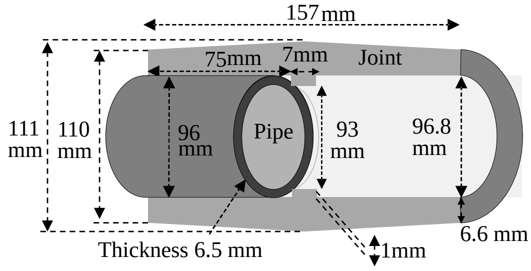

(b) Schematic of an adhesive joint with a pipe inserted on the left


(c) Photograph of the experimental setup

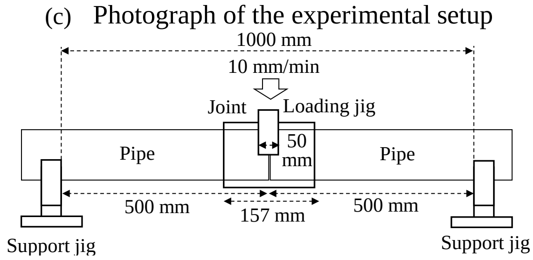

(d) Schematic of the experimental setup

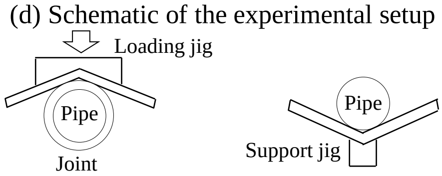

(e) Schematic of the loading and support conditions


(f) New pipe after the bending test


(g) Removed pipes after the bending test

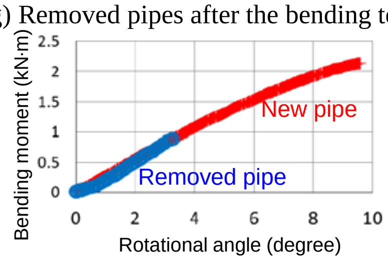

(h) Bending moment–rotational angle relationship

Fig. 1 Bending test [11]

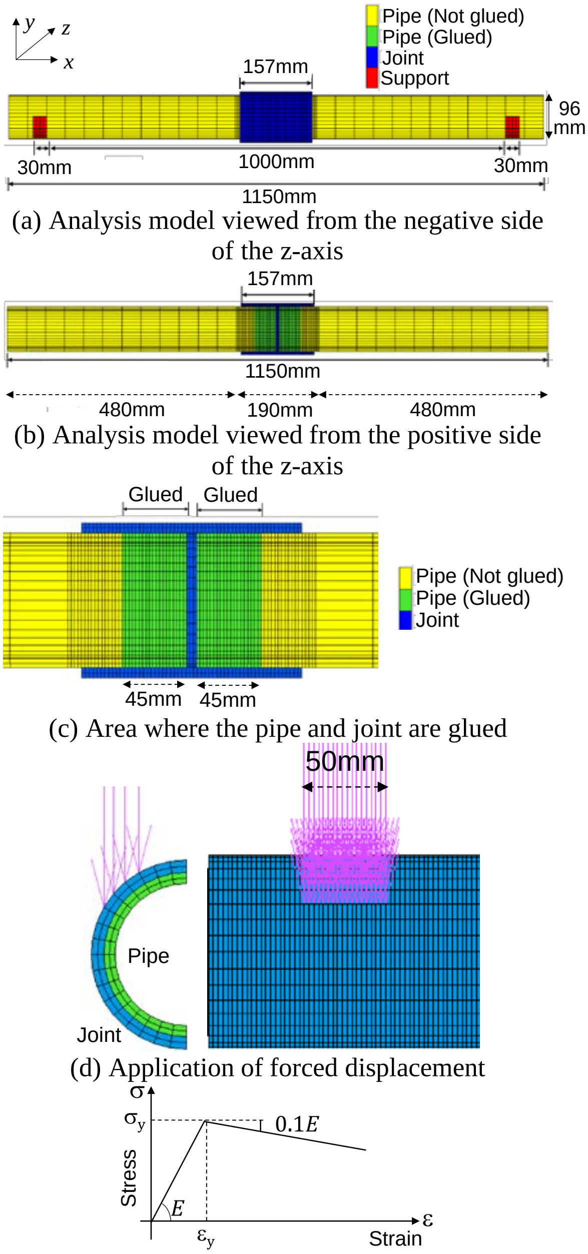

(a) Analysis model viewed from the negative side of the z-axis

(b) Analysis model viewed from the positive side of the z-axis

(c) Area where the pipe and joint are glued

(d) Application of forced displacement

(e) Stress–strain relationship (tension)

Fig. 2 Analysis model of the bending test

Figure 1(c) is a photograph of the experimental setup. The test specimen was supported at both ends by V-shaped steel jigs. Vertical displacement was forced at the top center of the test specimen in the downward direction at a speed of 10 mm/min by a V-shaped steel jig. Strain in the axial direction was measured at the top center and bottom center of the joint. Figure 1(d) is a schematic of the experimental setup, with dimensions given. Figure 1(e) illustrates how the vertical displacement was applied and how the test specimen was supported.

The bending test was conducted for newly created pipes (new pipes) and old pipes removed from the soil (removed pipes). Removed pipes were made during Japan's period of rapid economic growth between 1969 and 1982.

Photographs of new and removed pipes after bending tests are shown in Fig. 1(f) and (g). Figure 1(f) shows that the new pipe did not break but rather underwent plastic deformation. Figure 1(g) shows that the removed pipes broke. In the top photograph, the left pipe broke at the boundary between the part glued to the joint and the part not glued to the joint. In the bottom photograph, the joint broke in the middle.

Figure 1(h) shows the relationship between the bending moment and rotational angle for one new pipe and one removed pipe up to the maximum bending moment. This figure was derived from the force–displacement relationship. The figure shows that the new and removed pipes had similar stiffness, and the strength (maximum bending moment) of the removed pipe was less than half that of the new pipe. The strain observed during loading is presented later in the discussion of the analysis results.

3.3 Analysis Conditions

3.3.1 Analysis model

A three-dimensional static analysis of a bending test was performed using general-purpose finite element software, MSC Marc [13].

Figure 2(a) and (b) shows the analysis model as viewed from the negative and positive sides of the z-axis. Two pipes and a joint were modeled using eight-noded solid elements with a first-order interpolation. The two supports were modeled by four-noded rigid shell elements. A one-half region was modeled with the xy-plane being the plane of symmetry.

An actual joint has a tapered shape as shown in Fig. 1(b), but it was simply modeled as having a constant thickness of 6.5 mm. The projection at the center of the joint shown in Fig. 1(b) was modeled with a projection with a height of 1.5 mm so that the inner diameter at the center was 93 mm. The thickness of the pipe was set at 6.5 mm. The outer diameter of the pipe and the inner diameter of the joint were both set at 96 mm.

As shown in Fig. 2(b), the pipe was divided into elements having a length of 40 mm in 480-mm regions at both sides, and elements having a length of 2.5 mm in a 190-mm region at the center in the axial (x) direction. Both the pipes and joint were divided into two elements in the radial direction and 36 elements in the circumferential direction.

The supports were divided into elements of approximately 7.5 mm.

3.3.2 Interaction of the pipe, joint and supports

The interaction between each pipe and a joint and that between each pipe and a support was modeled using a contact analysis function.

Figure 1(b) shows that the tapered shape of the joint allows the pipe and joint to be glued more tightly near the center. Meanwhile, there is a gap between the pipe and joint at the entrance of the joint, and it is observed that the pipe and joint of the test specimen are not glued near the entrance of the joint. It is thus considered that the pipe and joint are not glued near the entrance of the joint.

On the above basis, the width of the glued region was set at 45 mm for each pipe as shown in Fig. 2(c). The pipe section shown in green in Fig. 2(c) was assumed to be glued to the joint. For this section, the pipe and joint were glued together and reacted against tensile, shear and compression stress until either the tensile or shear stress exceeded a threshold. If either the tensile or shear stress exceeded the threshold, the glue broke. Then, once broken, only compression and friction stresses were considered between the pipe and joint when in contact. The pipe section shown in yellow in Fig. 2(c) was assumed not to be glued to the joint and touch with the joint. For this section, only compression and friction stresses were considered between the pipe and joint when in contact.

It was assumed that the pipes and supports were not glued together and in touch. They interacted with compression and friction stress when in contact.

3.3.3 Boundary and loading conditions

Bounding conditions were that all nodes in the plane of symmetry were fixed in the z direction and all nodes belonging to the supports were fixed in all directions.

The loading condition was a vertical displacement applied to nodes where the V-shaped jig was in contact with the joint as shown in Fig. 2(d). The vertical load was computed by summing the reaction forces in the vertical direction.

3.3.4 Analysis parameters

The pipes and joint were made from PVC. The supports were assumed to be rigid.

The stress–strain relationship of PVC was modeled using the tension softening model shown in Fig. 2(e). Material properties of the PVC are given in Table 1(a). Young’s modulus, Poisson’s ratio, tension softening characteristics, and the tensile strength of new PVC were experimentally determined [14]. Figure 1(h) shows that the new and removed pipes had similar stiffness. Therefore, the same Young’s modulus, Poisson’s ratio, and tension softening characteristics were used for the new and removed pipes. Okutsu et al. [11] found no difference in strength between the new and removed pipes when testing specimens cut away from the joint. Meanwhile, as shown in Fig. 1(h), the maximum bending moment of the joint part of the removed pipe was half that of the new pipe. It is thus assumed that the strength of the removed pipe had deteriorated to half that of the new PVC only at the joint part.

Table 1 Analysis parameters of the bending test

(a) Material properties of PVC

Density	1440 kg/m^3
Young’s modulus *E*	2.45×10^6 kN/m^2
Poisson’s ratio	0.35
Tensile strength (new)	4.90×10^4 kN/m^2
Tensile strength (deteriorated)	2.45×10^4 kN/m^2

(b) Interaction between pipe and joint

Friction coefficient	0.3
Glue strength (normal direction)	2.0×10^4 kN/m^2
Glue strength (tangential direction)	2.0×10^4 kN/m^2

(c) Interaction between pipe and support

Friction coefficient	0.3

Table 1(b) gives the coefficient of friction between the pipe and joint and the strength of the glue. Table 1(c) gives the coefficient of friction between the pipe and support. Okutsu et al. [11] conducted a chemical analysis of glue taken from new and removed pipes and reported that the condition of the glue for the removed pipe was similar to that of the glue for the new pipe and that there was no observable deterioration of the glue. The same glue strength was thus used for the new and removed pipes.

3.4 Analysis Results

3.4.1 Relationship of the bending moment versus rotational angle

The analyzed load–displacement relationship was converted to the bending moment–rotational angle relationship. Figure 3(a) presents the bending moment–rotational angle relationship for the new and removed and new pipes. The circles indicate the times at which yielding first occurred. A comparison of Figs. 1(h) and 3(a) shows that the analysis and experimental results are in good agreement. The stiffness and bending moment when failure occurs are similar between the analysis and experimental results for both the new and removed pipes.

3.4.2 Relationship of the displacement versus strain

Figure 3(b) and (c) compares the displacement–strain relationships obtained in the experiment and analysis for the new and removed pipes. Three test results are shown for the experiments. Solid lines indicate the strain acting on the top of the center joint and dotted lines indicate the strain acting on the bottom of the center joint. The circles indicate the times at which yielding first occurred in the analysis. The displacement–strain relationship is seen to be accurately simulated for both the new and removed pipes.

3.4.3 Maximum principal stress distribution

Figure 3(d) and (e) shows the distribution of maximum principal stress for the new and removed pipes at which the bending moment is a maximum. The pipes yielded at the bottom near the boundary between the part glued to the joint and the part not glued to the joint, and at the joint at the center bottom.

3.4.4 Breaking of glue and the axial displacement distribution

Figure 3(f) and (g) shows the glued/contact situation between the pipe and joint for the new and removed pipes. Only the pipes are shown. Red indicates where the pipe is glued to the joint. Yellow indicates where the glue is broken or there was no glue initially, but the pipe is in touch with the joint. Blue indicates where the glue is broken or there was no glue initially, and the pipe is not in touch with the joint. The glue of the new pipe could be seen to break over a wider area than the glue of the removed pipe.

Figure 3(h) and (i) shows the axial displacements of the new and removed pipes. The new pipe is deformed in its entirety. In contrast, in the case of the removed pipe, the deformation is small inside the joint, and the pipe appears as if it undergoes rigid-body rotation outside the joint. This is because the damage is concentrated at the bottom of the pipe at the boundary between the

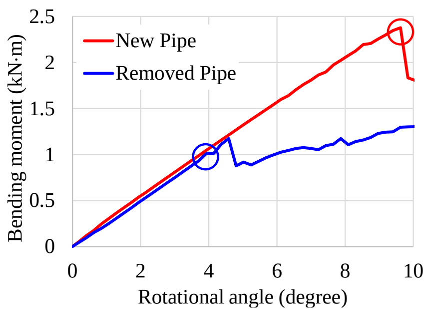

(a) Bending moment–rotational angle relationship [11]

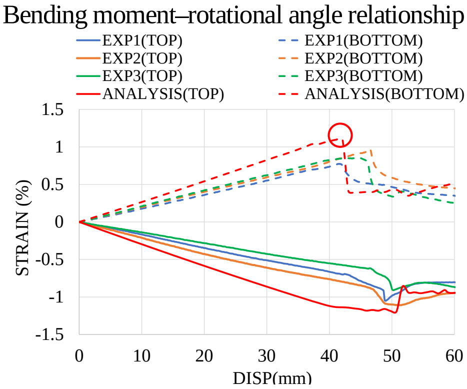

(b) Displacement–strain relationship for the new pipe [11]

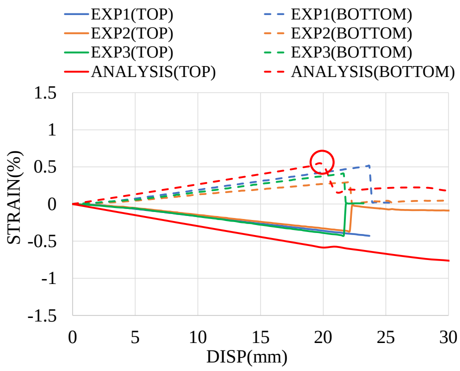

(c) Displacement–strain relationship for the removed pipe

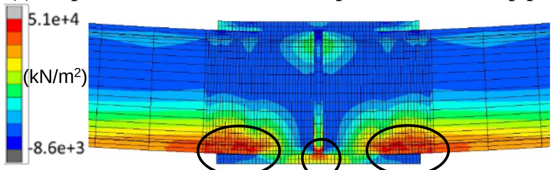

(d) Maximum principal stress at 40 mm for the new pipe

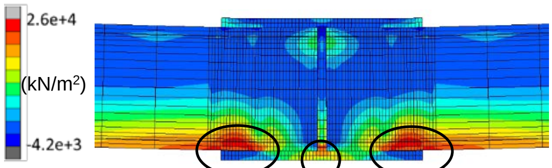

(e) Maximum principal stress at 20 mm for the removed pipe

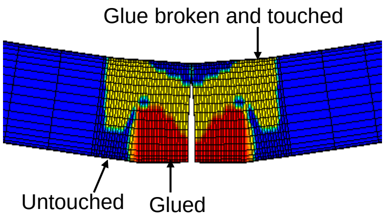

(f) Glued/contact condition at 80 mm for the new pipe

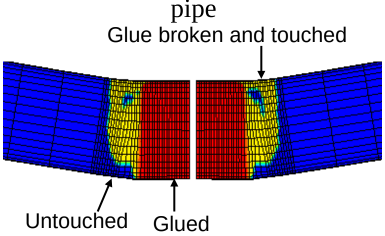

(g) Glued/contact condition at 80 mm for the removed pipe

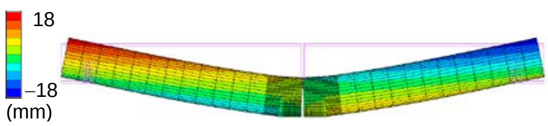

(h) Axial displacement at 80 mm for the new pipe

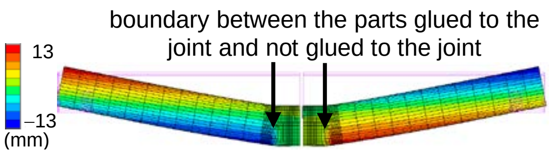

(i) Axial displacement at 80 mm for the removed pipe

Fig. 3 Analysis result of the bending test part glued to the joint and the part not glued to the joint. These findings are in agreement with Fig. 1(f), where the new pipe is entirely deformed, and with Fig. 1(g), where the removed pipe is ruptured at the boundary between the glued and non-glued parts.

The above results suggest that the analysis model of the pipes with an adhesive joint is reasonably well constructed.

4. DEVELOPMENT OF AN ANALYSIS MODEL OF THE SOIL–RIGID PVC PIPE INTERACTION THROUGH SOIL-TANK TEST SIMULATION

4.1 Overview

This section reports the development of an analytical model for the interaction between rigid PVC pipes and soil. The soil-tank test conducted by Okutsu et al. [12] was considered in a three-dimensional finite element analysis. The validity of the analytical model was verified by confirming the agreement of experimental and analytical results.

4.2 Soil Tank Test [12]

4.2.1 Experimental conditions

Figure 4 presents schematics of the soil-tank test. Rigid PVC pipes were installed in the soil tank, and forced displacement was applied to the pipes. The dimensions of the test specimen are given in the figure.

Three tests were conducted for three cases.

Case 1: One rigid PVC pipe without a joint subjected to forced displacement in the axial direction (z direction) (Fig. 4(a))

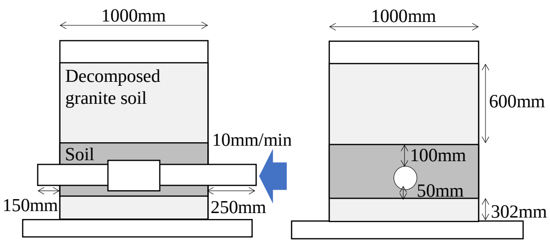

(i) Front view (ii) Side view
(a) Loading in the axial direction

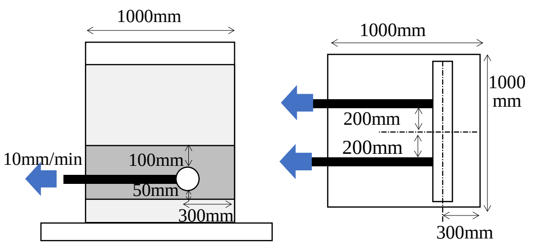

(i) Front view (ii) Top view
(b) Loading in the direction perpendicular to the pipe axis
Fig. 4 Soil-tank test [12]

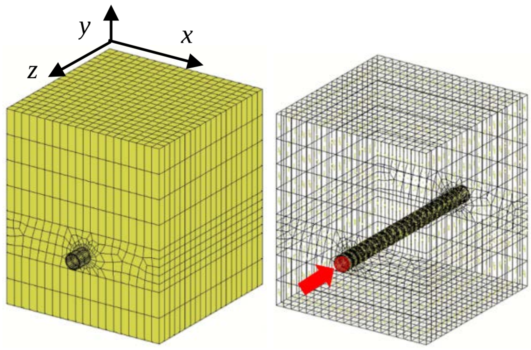

(i)Soil and pipe (ii)Pipe with the loading condition
(a) Loading in the axial direction with no joint (case 1)

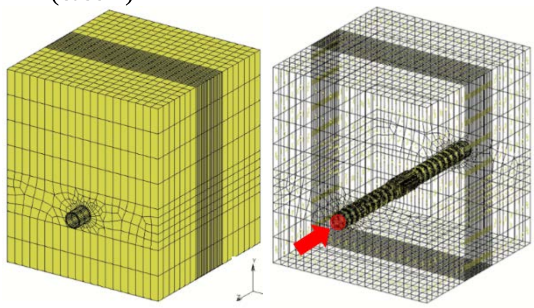

(i)Soil and pipe (ii)Pipe with the loading condition
(b) Loading in the axial direction with a joint (case 2)

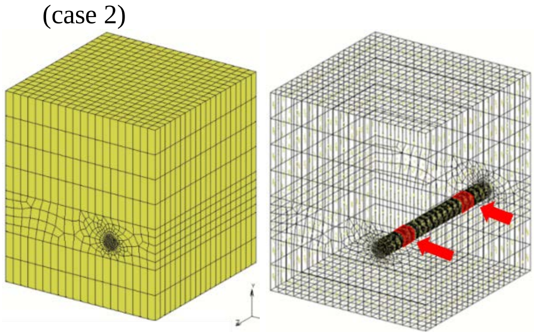

(i) Soil and pipe (ii)Pipe with the loading condition
(c) Loading in the direction perpendicular to pipe axis with no joint (case 3)

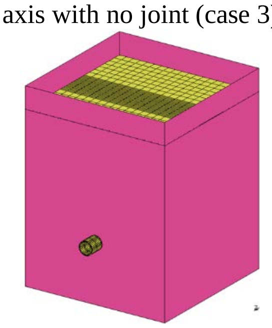

(d) Soil-tank, soil, and pipe

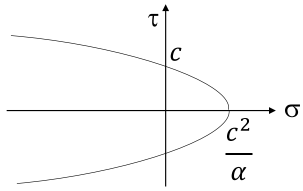

(e) Parabolic Mohr–Coulomb model
Fig. 5 Analysis model for the soil tank test

Table 2 Analysis parameters of the soil-tank test

(a) Material properties of the soil

Density	1850 kg/m^3
Young's modulus *E*	2.4×10^4 kN/m^2
Poisson's ratio	0.2
Bound strength c	17 kN/m^2
Tensile strength c^2/α	17 kN/m^2

(b) Coefficients of friction between soil and PVC and between the soil and tank

Soil – PVC	0.6
Soil - tank	0.3

Case 2: Two rigid PVC pipes with an adhesive joint subjected to forced displacement in the axial direction (z direction) (Fig. 4(b))

Case 3: One rigid PVC pipe without a joint subjected to forced displacement in the direction perpendicular to the pipe axis (x direction) (Fig. 4(c))

The force–displacement relationships were obtained for each of the cases and a comparison were made between the experimental and analysis results.

4.3 Analysis Conditions

4.3.1 Analysis model

Figure 5(a)–(d) presents the analysis model. The pipe and joint were modeled in a manner similar to the bending test. The soil was modeled with eight-noded rigid elements with a first-order interpolation and the tank was modeled with four-noded rigid elements.

In cases 1 and 3 without a joint (Fig. 5(a) and (c)), the model was divided into elements with length of 50 mm in the z direction. In case 2 with a joint (Fig. 5(b)), the model was divided into smaller elements with a length of 10 mm in the z direction where the joint existed.

In the height range from 50 mm below the bottom of the pipe to 100 mm above the top of the pipe, the model was divided into elements approximately 50 mm long in the x and y directions. In the remaining height range, the model was divided into elements 50 mm long in the x direction and 150 mm long in the y direction.

The nodes shown in red in Fig. 5(a), (b) and (c) are those where the forced displacement was added.

4.3.2 Analysis parameters

Analysis parameters of the pipes and joint are given in Table 1. The results for new and removed pipes are the same because there was no yielding of the pipes. Analysis parameters of the soil and the coefficients of friction between the soil and PVC and between soil and tank are given in Table 2. A parabolic Mohr–Coulomb model was adopted to model the material nonlinearity of the soil.

4.4 Analysis Results

Figure 6(a)–(c) compares the force–displacement relationship between experiment and analysis. In case 1 (Fig. 6(a)), the peak load is underestimated, but the yielding displacement and the final load have good agreement between the experiment and analysis. In cases 2 and 3 (Fig. 6(b)(c)), the force–displacement relationships have

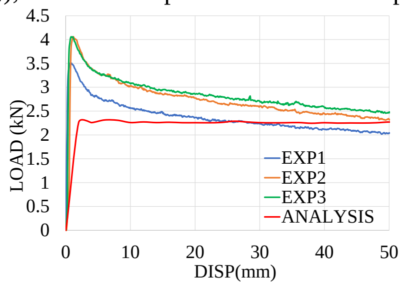

(a) Force–displacement relationship (case 1) [12]

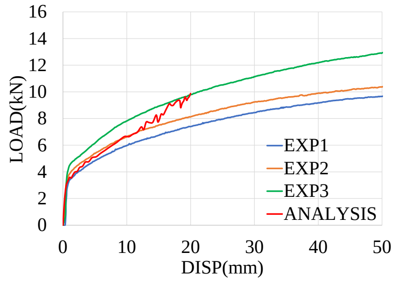

(b) Force–displacement relationship (case 2) [12]

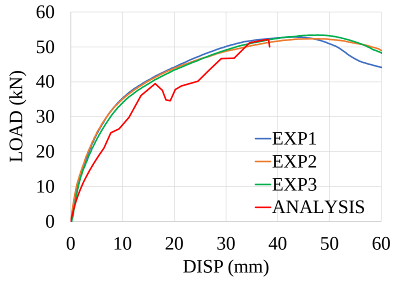

(c) Force–displacement relationship (case 3) [12]

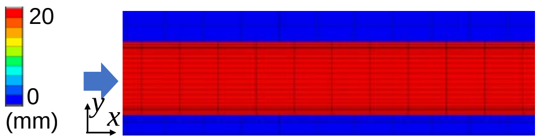

(d) Displacement in the x direction at 20 mm for case 1

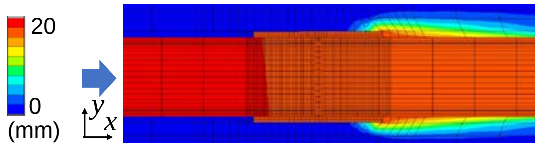

(e) Displacement in the x direction at 20 mm for case 2

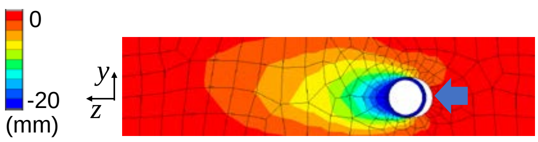

(f) Displacement in the z direction at 20 mm for case 3

Fig. 6 Analysis results of the soil-tank test good agreement between the experiment and analysis.

Figure 6(d)–(f) shows the distribution of displacement in the loading direction. In case 1 (Fig. 6(d)), only the pipe moves and the surrounding soil remains at its initial position. Only a frictional force acts between the pipe and soil in the x direction. Therefore, the load in Fig. 5(a) remains constant, which corresponds to the friction force. In case 2 (Fig. 6(e)), the joint pushes the soil on the right side of the joint in the x direction. Both a friction force and compression force act between the pipe and soil in the x direction. The load in Fig. 5(b) is thus greater than that in Fig. 5(a). In case 3 (Fig. 6(f)), both the pipe and joint push the soil on the left side. A compression force acts between the overall structure and soil. The load in Fig. 5(c) is thus much greater than that in Fig. 5(b).

The above results suggest that the analysis model for soil–pipe interaction is reasonably well constructed.

5. SAFETY EVALUATION OF RIGID PVC PIPES WITH AN ADHESIVE JOINT IN THE EVENT OF FAULT DISPLACEMENT

5.1 Analysis Conditions

This section reports on the evaluation of the safety of rigid PVC pipes with an adhesive joint in the event of fault displacement.

Figure 7(a), (b), and (c) presents the analysis model for two PVC pipes with an adhesive joint and the surrounding soil. The dimensions of the analysis model were 500 mm (width, x direction) × 500 mm (height, y direction) × 5000 mm (length, z direction). The fault plane was orthogonal to the pipe. Figure 7(d) presents three cases. In case I, the fault crosses the center of the joint. In case II, the distance between the center of the joint and the fault plane is 300 mm. In case III, the distance between the center of the joint and the fault plane is 500 mm.

In the z direction, the structural model (pipe and joint) was divided into elements with length of 25 mm around the joint and fault. In the remaining area, the structure was divided into elements with length of 200 mm. The soil model was divided in a similar manner in the z direction except for the fault area. At the location of the fault, the soil was divided into elements with length of 100 mm as shown in Fig. 7(b).

Figure 7(e) shows how the forced displacement was applied to the model in case I. Forced displacement was applied to the nodes in red in the downward direction and to the nodes in blue in the upward direction. The fault existed in the 100-mm yellow section between the red and blue parts.

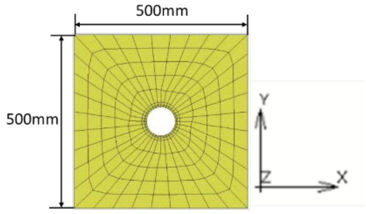

(a) Analysis model in the x–y plane

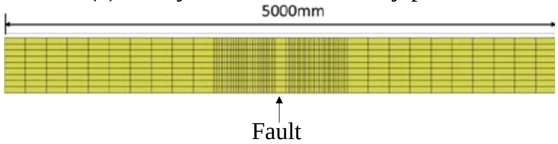

(b) Analysis model on the z–y plane (example of case I)

(c) Analysis model of the pipe and joint in the z–y plane (example of case I)

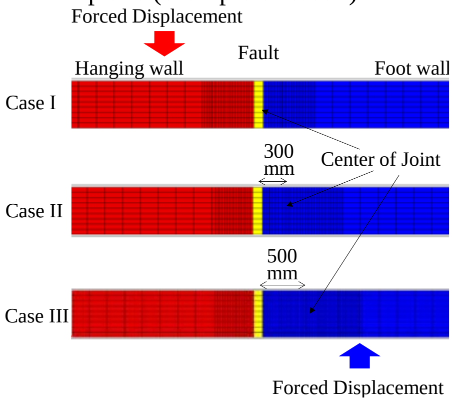

(d) Analysis cases with different fault locations

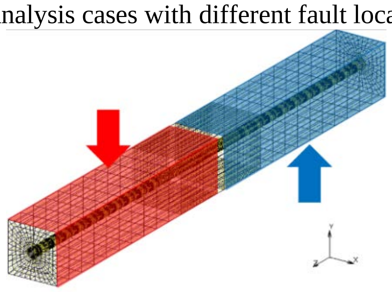

(e) Forced displacement applied to the nodes in red and blue (example of case I)

Fig. 7 Analysis model of fault displacement

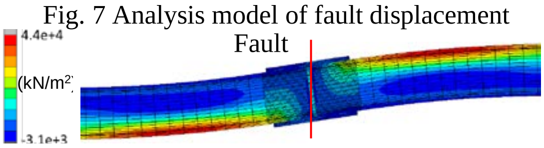

(a) Case I

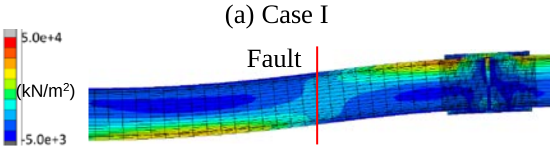

(b) Case II

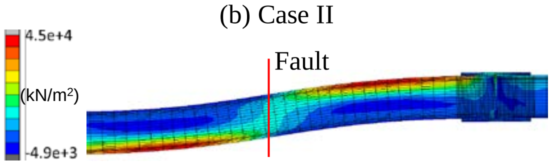

(c) Case III

Fig. 8 Maximum principal stress of a new pipe under fault displacement of 80 mm

5.2 Results for a Fault Crossing Angle of 90°

5.2.1 Maximum principal stress

Figure 8 shows the distribution of the maximum principal stress for new pipes under fault displacement of 80 mm. A similar tendency was observed for the removed pipes, and therefore only the results for the new pipes are shown.

In all cases, there is high maximum principal stress at a distance of 250 mm from the fault. In case I, there is high maximum principal stress in the pipes on both sides of the fault. In case II, there is high maximum principal stress in the joint on the right side and in the pipe on the left side of the fault. In case III, there is high maximum principal stress in the pipe and joint on the right side and in the pipe on the left side of the fault.

5.2.2 Plastic strain

Table 3 gives the fault displacement at which yielding occurred in the structure. Yielding occurs with the smallest fault displacement in case 2 for both the new and removed pipes.

In cases I and III, the yielding occurs at the same fault displacement of 90 mm for new pipes. However, for the removed pipe, there is yielding with smaller fault displacement in case III. This is because the yielding occurs in the pipe away from the joint for the new pipe and in the joint for the removed pipe.

Figures 9, 10, and 11 show the distribution of plastic strain in the axial direction (z). The blue area is where no yielding occurs. The nonblue area is where yielding occurs and the red area is where the largest plastic deformation occurs. In case I (Fig. 9), yielding occurs in the pipe away from the joint for the new pipe but at joint for the removed pipe because the removed pipe is weaker at the joint. In case II (Fig. 10), yielding occurs mainly at the joint and slightly at the pipe for the new pipe whereas yielding only occurs at the joint part for the removed pipe. The maximum plastic strain of the removed pipe (Fig. 10(b)) is approximately 12 times that of the new pipe (Fig. 10(a)). The plastic deformation due to fault displacement is thus concentrated at the weak joint for the removed pipe. In case III (Fig. 11), yielding occurs in the pipe for the new pipe and mainly at the joint and slightly at the pipe for the removed pipe.

In summary, the new pipe plasticizes at a distance of approximately 250 mm from the fault, and the plastic strain is a maximum when the joint is located in this area. The removed pipe tends to yield mainly at the joint regardless of the fault location. The plastic strain is a maximum when the joint is 300 mm from the fault.

5.3 Effect of the Fault Crossing Angle

Two other cases were analyzed to examine the effect of the fault crossing angle; namely, the reverse fault and normal fault cases with a fault crossing angle of 45° as shown in Fig. 12. The analysis was conducted only for the new pipe.

Table 4 summarizes the fault displacement at which yielding occurs. The fault crossing angle is 45°, and the vertical component of fault displacement is thus obtained by dividing the values given in Table 4 by $\sqrt{2}$.

Table 3 Fault displacement when yielding occurs (fault crossing angle of 90°)

Case	New pipe	Removed pipe
I	90 mm	85 mm
II	55 mm	25 mm
III	90 mm	50 mm

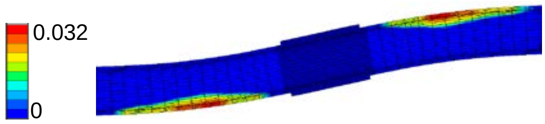

(a) New pipe

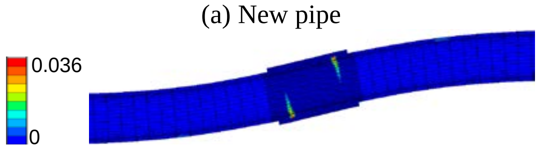

(b) Removed pipe

Fig. 9 Plastic strain in the axial direction at 120 mm for case I

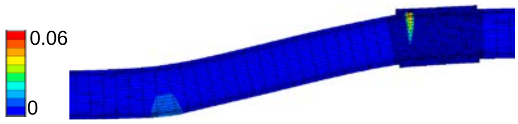

(a) New pipe

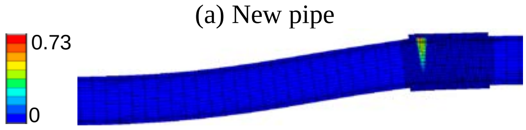

(b) Removed pipe

Fig. 10 Plastic strain in the axial direction at 80 mm for case II

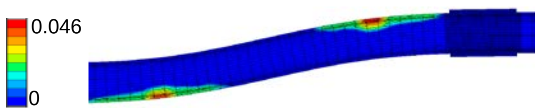

(a) New pipe

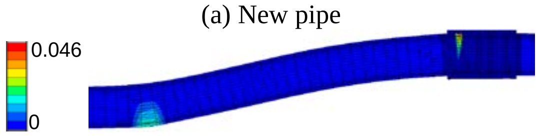

(b) Removed pipe

Fig. 11 Plastic strain in the axial direction at 120 mm for case III)

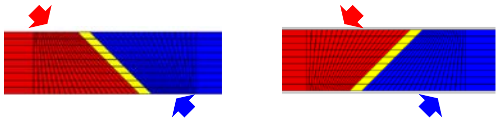

(a) Reverse fault (b) Normal fault

Fig. 12 Effect of the fault crossing angle

Table 4 Fault displacement at which yielding occurs for the new pipe

Case	Reverse fault (45°)	Normal fault (45°)
I	186 mm	180 mm
II	110 mm	82 mm
III	176 mm	152 mm

Yield occurs at the smallest fault displacement in case 2, for both reverse and normal faults. Yielding occurs with smaller fault displacement for the normal fault than for the reverse fault because the normal fault applies tensile stress to the structure in the axial direction.

A comparison of Tables 3 and 4 shows that the fault crossing angle of 90° has the severest impact on the structures. Table 3 shows that even a small displacement may cause serious damage to the old-standard rigid PVC pipes with an adhesive joint. Appropriate countermeasures such as repair thus necessary [15] [16].

6. CONCLUSIONS

This study evaluated the safety of old-standard rigid PVC pipes with an adhesive joints in the event of fault displacement in finite element analysis.

First, the analysis model of the rigid PVC pipes with an adhesive joint was developed in a numerical analysis of a bending test.

Next, an analysis model of the soil–pipe interaction was developed in a numerical analysis of a soil-tank test.

Then, fault displacements were input to an analysis model comprising rigid PVC pipes with an adhesive joint and surrounding soil. Yielding occurred at the joint with the smallest fault displacement of 55 mm for the new pipe and only 25 mm for removed pipes when the center of the joint was located 300 mm from the fault plane and the pipe was perpendicular to the fault plane.

The analysis shows that even a small displacement may cause serious damage to the old-standard rigid PVC pipes with an adhesive joint when the forced displacement acts in the direction perpendicular to the pipe axis. Appropriate countermeasures thus need to be taken.

7. ACKNOWLEDGMENTS

We thank Edanz (https://jp.edanz.com/ac) for editing a draft of this manuscript.

8. REFERENCES

[1] Moriya H., Komatsu S., Efforts at R & D of infrastructure technologies, the outline of infrastructure technologies supporting next generation networks, NTT technology journal, Vol. 18, Issue 3, 2006, pp.32-35. (in Japanese)

[2] Zhang Q., Okutsu M, Wakatake M., Suetomi M., Tsukamoto H., Shoji G., Suzuki T., Damage tendency analysis on telecommunication conduits due to past strong inland earthquakes, Journal of Japan Society of Civil Engineers, Ser, A1 (Structural Engineering & Earthquake Engineering (SE/EE)), Vol. 74, Issue 4, 2018, pp. I_1062-I_1069.

[3] Ito A., Okutsu M., Suetomi I., Tsukamoto H., Suzuki T., Damage analysis of rigid PVC pipe and steel pipe for communication, Journal of Japan Society of Civil Engineers, Ser, A1 (Structural Engineering & Earthquake Engineering (SE/EE)), Vol. 76, Issue 4, 2020, pp. I_552-I_558.

[4] Newmark N.M., Hall W.J., Pipeline design to resist large fault displacement, Proceedings of the U.S. national conference on earthquake engineering, 1975, pp.416-426.

[5] Kennedy R.P., Chow A.W., Williamson R.A., Fault movement effects on buried oil pipeline, ASCE, Journal of Transportation Engineering, Vol. 103, 1977, pp.616-633.

[6] Takada S., Fukuda K., Hassani N., Propose of simplified design method for buried pipes crossing earthquake fault, Journal Japan Society of Civil Engineers, Vol. 2001, Issue 668, 2001, pp.187-194. (in Japanese)

[7] Miyajima M., Yoshifuji Y., Kitaura M., Experiments on behavior of buried pipe due to surface fault rapture by using shear soil box, Journal of Earthquake Engineering, JSCE, Vol.27, No.104, 2003. (in Japanese)

[8] Takada S, Nakano M, Katagiri S, Tani K, Koyanagi S, Experimental study on earthquake-proof u-PVC pipeline subjected to uneven ground settlement during earthquakes, Journal of JSCE, Vol. 1999, Issue 619, 1999, pp. 145-154. (in Japanese)

[9] Hassani R., Basirat R., A 3D numerical modeling of polyethylene buried pipes affected by fault movement, Engineering Science and Technology, an International Journal, Vol. 22, Issue 2, 2019, pp. 482-488.

[10] Tsatsis A., Loli M., Gazetas G., Pipeline in dense sand subjected to tectonic deformation from normal or reverse faulting, Soil Dynamics and Earthquake Engineering, Vol. 127, 2019, 105780.

[11] Okutsu M, Kanetsugi M, Wakatake M, Katagiri S, Suzuki T, Basic study on characteristics of adhesive joint used for earthquake resistance evaluation of existing rigid PVC pipe, Proceedings of the symposium on disaster mitigation and resilience of the infrastructures and lifeline systems, 2018. (in Japanese)
[12] Okutsu M, Ito A., Itasaka K., Katagiri S., Experimental study on ground spring for PVC pipe for communication, Proceedings of the symposium on disaster mitigation and resilience of the infrastructures and lifeline systems, 2021. (in Japanese)
[13] MSC Software Corporation, Marc Volume A Theory and User Information 2018.
[14] Yokota T., Ogawa F., Fukatani W., Suehisa M., Miyamoto T., Nozawa M., Kaya T., Study on developing criteria for abnormality and urgency classification of polyvinyl chloride pipes, Technical NOTE of National Institute for Land and Infrastructure Management, No. 878, 2015. (in Japanese)
[15] Garrido M., Antonio D., Lopes J.G., Correia, J. R., Reparability of aged PVC waterproofing membranes: Effect of joining method, Journal of Building Engineering, Vol.33, 2021, 101569.
[16] Taleyarkhan R.P., Hemesath M., Jiang W., Rushford L., PLA wear layer based luxury vinyl tiles-Construction and characterization for adhesion strength and wear vs PVC, International Journal of Adhesion and Adhesives, Vol,117, 2022, 103170.